

Periodontal tissue engineering by transplantation of multilayered sheets of phenotypically modified gingival fibroblasts

K. Nakajima, T. Abe, M. Tanaka, Y. Hara

Department of Periodontology, Unit of Translational Medicine, Course of Medical and Dental Sciences, Nagasaki University Graduate School of Biomedical Sciences, Nagasaki, Japan

Nakajima K, Abe T, Tanaka M, Hara Y. Periodontal tissue engineering by transplantation of multilayered sheets of phenotypically modified gingival fibroblasts. J Periodont Res 2008; 43: 681–688. © 2008 The Authors. Journal compilation © 2008 Blackwell Munksgaard

Background and Objective: In periodontal tissue engineering, the sourcing of most of the relevant cells is limited by poor accessibility, whereas the use of readily available gingival fibroblasts is hampered because of their inhibitory effects on bone formation. To address the latter drawback, we developed a new graft composed of fibronectin (FN) matrix-based multilayered cell sheets of human gingival fibroblasts modified to express alkaline phosphatase (ALP). This study was undertaken to investigate the effects of this graft, called the FN-ALP transplant, on the healing of periodontal defects in a rat model.

Material and Methods: The FN-ALP transplants were grafted into periodontal fenestration bone defects in immunosuppressed rats. The process of periodontal healing was examined by histology, histomorphometry and immunohistochemistry. Grafted cells were tracked by immunostaining with human-specific antibodies. Control groups included non-transplanted empty defects and defects to which cell sheets without ALP induction had been grafted.

Results: After implantation, the FN-ALP transplants healed alveolar bone defects by intramembranous ossification, with formation of cementum and periodontal ligament. Moreover, FN-ALP transplants increased new bone formation, by endochondral ossification, on the mandibular cortex adjacent to the defect. Grafted fibroblasts were located near host osteoblasts and chondrocyte precursor cells early in the ossification process but were undetectable on and in newly formed bone and cartilage.

Conclusion: These results indicate that the FN-ALP transplants support alveolar bone regeneration within the defect and augment bone formation outside the defect through the recruitment of host osteo/chondrogenic cells, suggesting their potential for periodontal tissue engineering applications.

Tatsuya Abe, Department of Periodontology, Unit of Translational Medicine, Course of Medical and Dental Sciences, Nagasaki University Graduate School of Biomedical Sciences, 1-7-1 Sakamoto, Nagasaki 852-8588, Japan
Tel: 095 819 7683
Fax: 095 819 7684
e-mail: tabe@net.nagasaki-u.ac.jp

Key words: tissue engineering; periodontal regeneration; cell transplantation; alkaline phosphatase

Accepted for publication November 16, 2007

Periodontitis, a major cause of tooth loss in adults, destroys the tooth-supporting tissues, including the gingiva, periodontal ligament (PDL), cementum and alveolar bone (1). Current periodontal therapies are effective in regenerating these structures to a limited extent (2,3). Tissue engineering offers a promising new approach to regenerating lost periodontal tissues (2–4). Producing a graft with easily available, patient's own cells helps facilitate clinical application. In periodontal tissue engineering, however, the sourcing of most of the relevant cells is limited by supply and donor site morbidity. For example, tooth extraction is needed to harvest PDL cells, the best-studied graft cells in animal models of periodontal engineering (5). We decided to use gingival fibroblasts because they are a readily accessible, autologous cell source with little donor-site morbidity. Given that successful periodontal regeneration requires bone formation, a problem in grafting fibroblasts is that they decrease or inhibit bone formation (6). To circumvent this problem, we developed a new graft composed of fibronectin (FN) extracellular matrix (ECM)-based multilayered sheets of human gingival fibroblasts modified to express alkaline phosphatase (ALP). The design of our graft is based on the hypothesis that *in vitro* phenotypic modification or activation of graft fibroblasts improves their capacity for periodontal healing.

Expression of ALP is induced in gingival fibroblasts during inflammation *in vivo* (7) and matrix formation *in vitro* (8), suggesting the relevance of ALP induction to fibroblast activation. The biological functions of ALP other than its promotion of calcification by hydrolyzing pyrophosphate, an inhibitor of mineralization (9,10), remain unknown. We previously showed that serum-free ascorbic acid stimulation induces ALP in gingival fibroblasts *in vitro*, depending on FN (11). Fibroblasts are biologically active in FN matrices (12). To engineer an FN-based graft, we used a culture system in which transforming growth factor- β (TGF- β 1) stimulates fibroblasts to form a multilayered sheet in

the self-produced FN ECM (13). Recent studies have shown that PDL cell sheets can regenerate periodontal tissues in animal models (14,15). However, there is little information on the use of multilayered gingival fibroblast sheets for periodontal tissue engineering.

In this study, we investigated the effects of the FN-based, ALP-expressing human gingival fibroblast transplant on the healing of periodontal fenestration bone defects in rats. We report here that this new transplant not only supports alveolar bone regeneration but also increases bone formation.

Material and methods

Cells, multilayer formation and ALP induction

Fibroblasts were obtained from explants of clinical healthy gingival tissues taken from nine patients (aged 34–54 years) undergoing periodontal surgery, following an institutional review board-approved protocol. All of the patients participated after providing written informed consent. The cells were grown in α -minimal essential medium (α -MEM; GIBCO BRL, Grand Island, NY, USA) supplemented with 10% fetal bovine serum (FBS) and antibiotics (100 U/mL penicillin and 100 μ g/mL streptomycin) in a humidified 95% air and 5% CO₂ incubator at 37°C. Cells were used between passages four and six.

Cells were seeded on human plasma FN-coated 24- or six-well tissue culture plates (Falcon; Becton Dickinson, Lincoln Park, NY, USA) at subconfluence (3×10^4 cells/cm²) and allowed to grow to confluence in α -MEM with 10% FBS and antibiotics. The confluent cells were then grown into multilayered cell sheets in a chemically defined S-Clone medium (Sanko Junyaku, Tokyo, Japan; 11) containing 1 ng/mL human plasma TGF- β 1 (R&D Systems, Minneapolis, MN, USA), 0.15 mM L-ascorbic acid 2-phosphate (AsAP; Wako, Osaka, Japan), 10% FBS and antibiotics for 6 days, as described previously (13). Subsequently, the multilayered cells were treated with ALP induction

medium (serum-free S-Clone medium with AsAP, 0.1 ng/mL TGF- β 1 and antibiotics; 11) for an additional 4 days. The medium was changed every 2 days.

In vitro assays for cell numbers, ALP activity and FN deposition

The DNA content was measured by a Hoechst 33258 dye assay. Alkaline phosphatase activity was measured by the colorimetric assay using *p*-nitrophenyl phosphate (Sigma, St Louis, MO, USA) and expressed as nanomoles of *p*-nitrophenol (*p*-NP) liberated per minute per well (11). Cells were stained for ALP activity in the 5-bromo-4-chloro-3-indolyl phosphate (BCIP)-nitro blue tetrazolium (NBT) mixture (Sigma; 11). With added levamisole, an inhibitor of ALP, the control cells did not show any reaction product. Immunostaining with a mouse monoclonal antibody (mAb) to cellular FN (1:400 dilution, DH1; Locus Genex, Helsinki, Finland) was carried out using a Vectastain Universal Quick Kit (Vector, Burlingame, CA, USA; 11).

Graft preparation and transplantation

For transplantation, cell sheets in six-well plates were cut into small rectangles (7 mm \times 8 mm) and gently detached from the well with Teflon-coated forceps. They were immediately covered with a bovine serum albumin (BSA)-coated coverglass, kept settled on the well, and cultured to maintain cell viability. The prepared transplants were grafted into rats within 2 h. The number of viable cells per transplant was estimated to be $9.5 \pm 2.6 \times 10^4$ cells by a Neutral Red assay (11), using the replica of each graft in parallel cultures.

Animal experiments followed the protocol approved by the Animal Care and Use Committee of Nagasaki University. Seven- or 8-wk-old male Wistar rats weighing 230–270 g were used. Periodontal fenestration bone defects were created at the left mandible of each rat as described previously (16). Briefly, rats were anesthetized by intraperitoneal injection of 0.5 mg/kg Nembutal (Dainippon Sumitomo

Pharma, Osaka, Japan). After an extra-oral incision at the base of the left side of the mandible and dissection of muscle, the buccal mandibular bone overlying the first molar roots was drilled to create a defect with a size 4 round dental burr under saline irrigation. The exposed tooth roots were carefully denuded of PDL, cementum and superficial dentin. After rinsing with serum-free medium to prevent transfer of serum and additives, a single transplant was placed *en block* into each defect. The muscle was repositioned and the skin was sutured closed with 4-0 polyglycolic acid sutures. The immunosuppressant FK506 (1 mg/kg body weight; Astellas, Tokyo, Japan) was intramuscularly administered to the rats every day for the first 2 wks and every other day for an additional 2 wks after surgery, as described previously (17,18). Rats were killed at 5, 10, 14 and 28 days after implantation. In addition to the above experimental group ($n = 12$, three per time point), three control groups included 5, 10, 14 and 28 day non-transplanted empty defects ($n = 12$), 14 day empty defects without FK506 administration ($n = 3$) and 14 day defects to which cell sheets without ALP induction had been grafted ($n = 3$).

Histology and histomorphometry

After intracardiac perfusion fixation with 4% paraformaldehyde, the mandible was removed and immersed in the same fixative for 1 h at 4°C. The specimens were decalcified with 10% EDTA at 4°C and embedded in paraffin. Serial horizontal 6- μ m-thick sections were cut in the apical-to-coronal direction of the tooth, as described previously (16). Hematoxylin and Eosin (H&E) staining was performed on every fifth section through the region of the defect. The other sections were either stained with Alcian Blue or processed for immunohistochemical staining.

For histomorphometry, we used H&E sections taken at three different locations separated by about 100 μ m intervals through the middle of the defect. Using images of the sections taken with a digital camera, the pro-

portion of total new bone area in the defect was determined by processing the images in Adobe Photoshop as described previously (19). We measured the thickness of newly formed bone and cartilage on the original cortical bone every 1/8 defect-width (W) interval between a defect edge and a point being one W away from the edge, using light micrographs printed at a magnification of $\times 82$. The results were expressed as the average thickness. Newly formed bone was identified in the pictures and prints by their differential staining of Eosin and by the woven structure, with bone sialoprotein (BSP)-immunostained adjacent sections for reference.

Immunohistochemistry

Immunostaining with mouse mAbs to CD44 (at the ready; 156-3C11; Lab Vision, Fremont, CA, USA) and tenascin-C (TN-C; 1:100 dilution; DB7; Locus Genex) was carried out using a Vectastain ABC-AP kit (Vector) with an Avidin/Biotin Blocking Kit (Vector) and a secondary antibody pre-absorbed with normal rat serum, according to the manufacturer's instructions. The enzyme activity was visualized using Vector Red (Vector) in conjunction with a levamisole solution (Vector). For prior CD44 antigen retrieval, sections were gradually heated up to 74°C from 37°C in 10 mM sodium citrate buffer (pH 6.0) for 3 h with a thermal controller. We found that this heat treatment was as effective in epitope recovery as and gave more excellent tissue preservation than a routine microwave method (Nakajima K and Abe T). We checked the human specificity of the anti-CD44 and anti-TN-C mAbs by immunostaining empty defect groups and found no reaction product in the control sections. A standard indirect immunoperoxidase staining was performed with rabbit polyclonal antibody to BSP (1:100 dilution; Chemicon, Temecula, CA, USA) and rabbit antiserum against the N-terminal residues of human tissue non-specific ALP (1:100 dilution; 20). Peroxidase activity was visualized with 3,3'-di-

aminobenzidine tetrahydrochloride and H₂O₂. We checked immunostaining specificity by replacing the primary antibody with normal mouse or rabbit immunoglobulin G and found no reaction product in the control sections.

Statistics

Each experiment was performed three times independently using fibroblasts obtained from different donors and each was assayed in triplicate wells. Data are presented as means \pm SD. Statistical analyses were performed by one-way analysis of variance (ANOVA) followed by Tukey's *post hoc* test.

Results

Production of ALP-expressing fibroblast multilayered sheets

Treatment of confluent monolayers with TGF- β 1 in the presence of AsAP and FBS for 6 days resulted in multilayered cell sheet formation. Transfer of the stratified cells to AsAP with a lower dose of TGF- β 1 for an additional 4 days significantly increased the ALP activity, with no changes in cell numbers as determined by total DNA (Fig. 1A). In these cultures, almost all of the cells were ALP positive (Fig. 1B). Immunostaining showed a dense deposition of cellular FN between cells in cultures both with and without ALP induction (data not shown). We refer to grafts prepared from the cultures with and without ALP induction as FN-ALP and non-ALP transplants, respectively (Fig. 1C).

Effect of FN-ALP transplants on periodontal healing

After being grafted into rat periodontal fenestration defects, the FN-ALP transplants induced intramembranous ossification within the defects and endochondral ossification on the original cortical bone adjacent to the defects. We describe these two bone formation events separately. Since there was no difference in healing be-

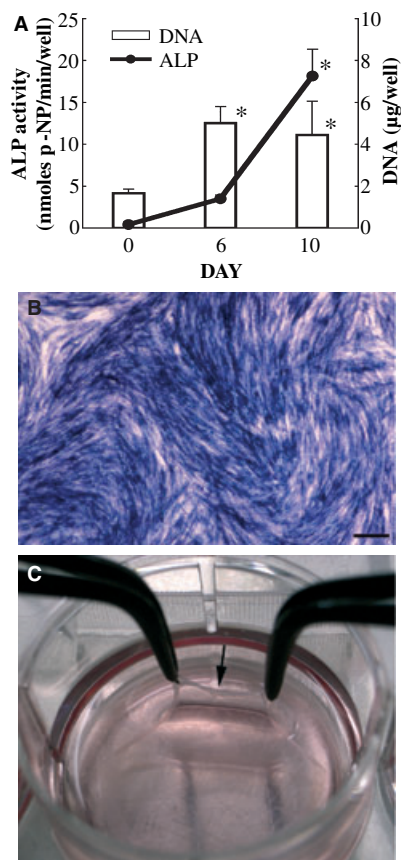


Fig. 1. Alkaline phosphatase induction and cell growth *in vitro*. Confluent fibroblasts in 24- or six-well plates were treated with 1 ng/mL TGF- β 1, 0.15 mM AsAP and 10% FBS for 6 days and then incubated in AsAP and 0.1 ng/mL TGF- β 1 for an additional 4 days (day 10). The cells in 24-well plates were assayed for ALP activity and DNA content (A). Results are the means \pm SD of three independent experiments. * Significantly higher than values at day 0 ($p < 0.01$). The cultures on day 10 were stained for ALP activity (blue; B) and not counterstained. Similar results were obtained in three independent experiments. Scale bar represents 200 μ m. (C) Appearance of a 10 day cell sheet (arrow) in a six-well plate.

tween empty defect groups with and without FK506 (data not shown), we describe the results for only the former group.

Intramembranous bone formation within periodontal defects The process of rat periodontal defect healing followed sequential phases, including inflammation and granulation tissue (day 5), early intramembranous ossification

(day 10), bone filling (day 14) and bone maturation stages (day 28), as described previously (21). On day 14, the defect had been filled with newly formed woven bone in the FN-ALP transplant group, whereas fibrous tissue, with limited bone formation, had been produced in the defect in the non-ALP transplant group (Fig. 2A,B). The empty defect group showed bone filling (Fig. 2C). The new bone was positive for BSP, a marker for newly mineralized tissues (data not shown; 22). Similar results were obtained in three independent experiments. On day 14, the proportion of new bone area in the defect (including PDL regions) in the FN-ALP transplant group was significantly ($p < 0.01$) higher than that in the non-ALP transplant group and was similar to that in the empty group (Fig. 2D). The border between new and original

was well defined by day 14 but often indistinguishable on day 28 because of bone maturation.

Endochondral bone formation on cortical bone On day 5, the mandibular cortex near the defect was covered with fibrin and a few cells in both the FN-ALP transplant and the empty groups (data not shown). On day 14, prominent bone and cartilage tissues were observed on the original cortical bone both anterior and posterior to the defect in the FN-ALP transplant group (Fig. 3A). These newly formed tissues contained many round hypertrophic chondrocytes and were positive for Alcian Blue, indicating endochondral ossification (Fig. 3B,C). These tissues were covered with numerous mesenchymal cells (Fig. 3A). Trabecular bone with bone marrow developed between the cartilage and the original

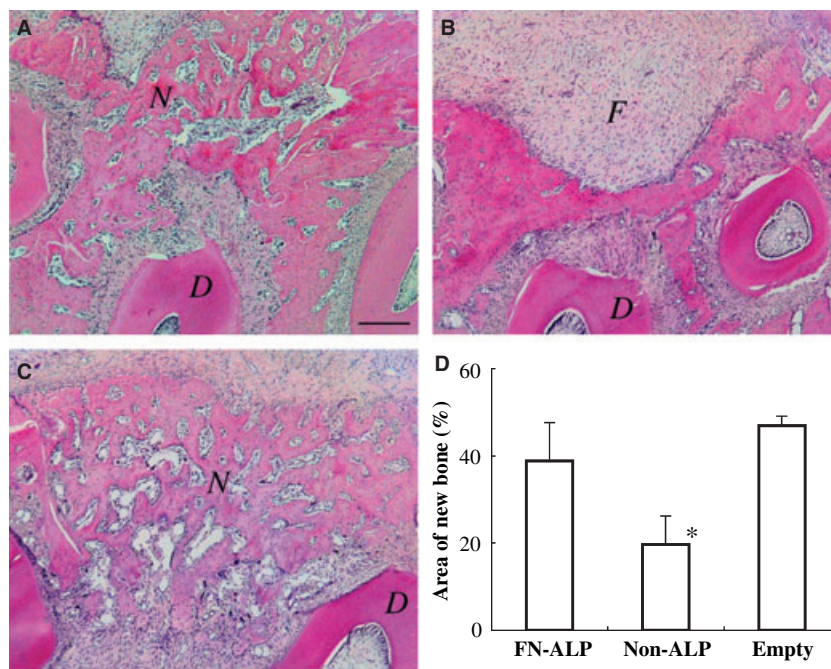


Fig. 2. Intramembranous bone formation in periodontal defects. Rats received either FN-ALP transplant or non-ALP transplant in periodontal fenestration defects or did not receive any transplant (empty defects). The light micrographs shown were taken from H&E sections of an FN-ALP transplanted (A), non-ALP transplanted (B) or non-transplanted empty group (C) at 14 days. N, new bone; F, fibrous tissue; and D, tooth dentin. Similar results were obtained in three independent experiments. Scale bar represents 200 μ m. (D) Total new bone area in the defect (including PDL regions) in FN-ALP transplant (FN-ALP), non-transplanted (empty), and non-ALP transplant (non-ALP) groups at 14 days. Results are the means \pm SD of three independent experiments. *Significantly lower than FN-ALP ($p < 0.01$). No significant difference was observed between FN-ALP and empty groups ($p > 0.05$).

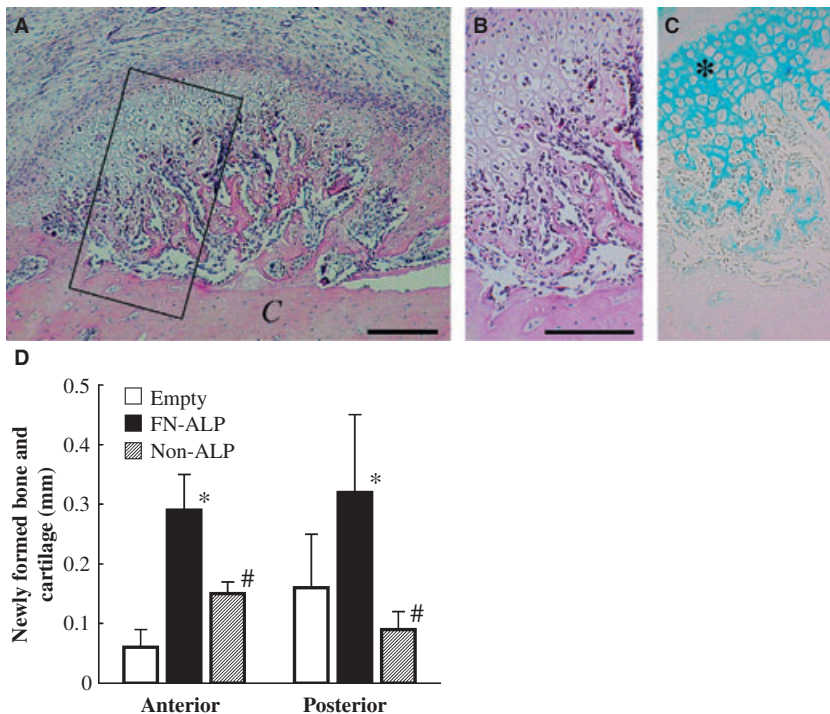


Fig. 3. Endochondral bone formation on the original cortical bone. Rats received either FN-ALP transplant or non-ALP transplant in periodontal fenestration defects or did not receive any transplant. (A) A light micrograph of newly calcified tissues on the mandibular cortex (C) adjacent to the defect at 14 days after grafting an FN-ALP transplant. H&E staining. Scale bar represents 200 μ m. (B) Detail of the cartilage and trabecular bone shown in the rectangular area in (A). Scale bar represents 200 μ m. (C) An Alcian Blue (*) section adjacent to (B). Similar results were obtained in three independent experiments. (D) The thickness of newly formed bone and cartilage on the mandibular cortex both anterior and posterior to the defect in non-transplanted (empty), FN-ALP transplant (FN-ALP) and non-ALP transplant (non-ALP) groups at 14 days. Results are the means \pm SD of three independent experiments. *Significantly higher than empty ($p < 0.01$); #Significantly lower than FN-ALP ($p < 0.01$).

cortex (Fig. 3A,B). Similar results were obtained from three independent experiments. In morphometric analysis, the average thickness of newly formed bone and cartilage both anterior and posterior to the defect was significantly ($p < 0.01$) larger in the FN-ALP transplant group than in either the empty defect or non-ALP transplant group (Fig. 3D). There were no differences in the defect width (2.1 ± 0.38 mm) among the three groups.

Cementum and PDL formation on denuded tooth roots We examined the formation of cementum and PDL after grafting FN-ALP transplants. No mineralized tissues were seen on the cut dentin by day 14. On day 28, a thin layer of an eosinophilic tissue, which was BSP positive, was observed along

the denuded dentin surface, indicating cementogenesis (Fig. 4A,B; 22). The PDL tissue was well organized with collagen fibers extending between new cementum and alveolar bone (Fig. 4C). Neither ankylosis nor root resorption was seen on the cut dentin at any time point examined. Similar results were obtained from three independent experiments. The empty group, like FN-ALP group, showed a thin layer of new cementum along the denuded dentin on day 28 (Fig. 4D).

Localization of grafted FN-ALP transplants

We tracked grafted FN-ALP transplants by immunostaining of the donor cells and matrices with human-specific mAbs to CD44 and TN-C, respectively.

The cell-surface adhesion molecule CD44 is widely used as a marker for the mesenchymal cell lineage (23), and the ECM protein TN-C is expressed throughout the course of wound healing (24). In serial sections, there were parallels between the distribution patterns of CD44-positive cells and TN-C-positive matrices throughout the time periods studied. On day 5, CD44-positive cells were distributed throughout the defect area (Fig. 5A,B). On day 10, CD44-positive cells and TN-C-positive matrices were located in soft tissues in the defect (Fig. 5C–E). Marker-positive grafted cells/matrices were undetectable on and in newly formed bone and cartilage at any time point examined (Fig. 5D,E). On days 14 and 28, a few CD44-positive cells were sometimes found scattered in the area of the former defect (data not shown). The FN-ALP group, like the empty group (data not shown), showed little inflammatory cell infiltration into the defect after day 10. We examined ALP expression by immunostaining with a specific antibody that cross-reacts with rat ALP. The CD44-positive cells displayed no or weak ALP staining at any time point examined (Fig. 5C,F). Osteoblasts and chondrocyte precursor cells, which were gathered on newly formed bone and cartilage, strongly expressed ALP, but not CD44, in the vicinity of CD44-positive cells (Fig. 5C,D,F).

Discussion

In this study, we show that transplantation of FN-based multilayered sheets of ALP-expressing human gingival fibroblasts promotes bone formation in a rat periodontal fenestration defect model. The transplants supported alveolar bone regeneration via intramembranous ossification and augmented endochondral bone formation on the cortical bone. The grafts also led to the formation of PDL and cementum on the denuded dentin surface. These results suggest the potential of the FN-ALP transplants for periodontal tissue engineering applications. Gingival fibroblasts are easy to harvest with little donor-site morbidity. Thus, FN-ALP transplants are constructed

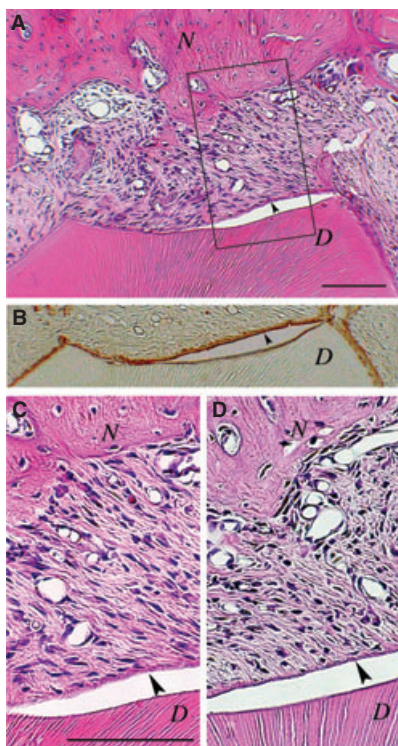


Fig. 4. Cementum and PDL formation. Rats received FN-ALP transplants in periodontal fenestration defects or did not receive any transplant. (A) A light micrograph of the PDL region of an FN-ALP transplant group at 28 days. A thin layer of cementum (arrowhead) is seen along the cut dentin (*D*) surface. The split between the new cementum and cut dentin surface is an artifact produced during histological preparation. H&E staining. *N*, new bone. Scale bar represents 100 μ m. (B) Immunostaining for BSP of a section adjacent to (A). Reaction product (arrowhead, brown) is seen along new and original cementum. Not counterstained. (C) Magnification of the rectangular area in (A). Scale bar represents 100 μ m. (D) A light micrograph of the PDL region of an empty group rat at 28 days. H&E staining. Similar results were obtained in three independent experiments.

with autologous cells, which eliminate the risks of graft rejection and disease transmission. The FN-based cell sheets are malleable, allowing flexible fitting into alveolar bone defects. The grafts could be applied to a weight-bearing site if combined with a solid support.

We chose the rat periodontal defect model because it is one of the most popular animal models for reliable

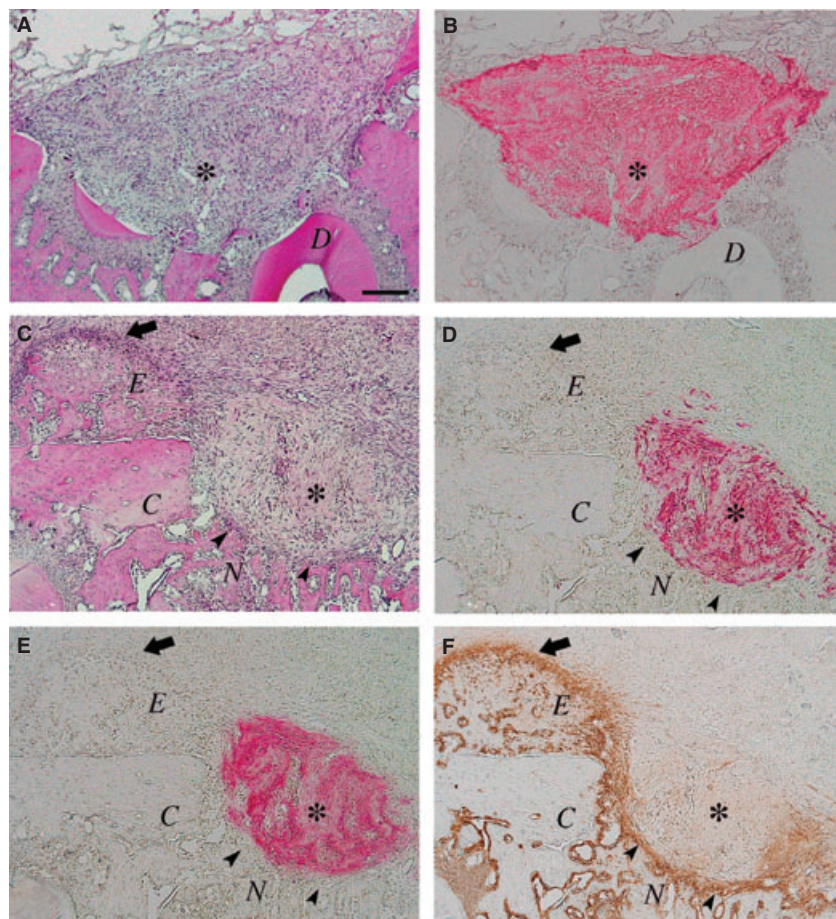


Fig. 5. Tracking of transplanted cells. Rats received FN-ALP transplants in periodontal fenestration defects. (A,B) Serial sections obtained at 5 days were subjected to H&E staining (A) or immunostaining for CD44 (B). The CD44-immunopositive cells (red) are distributed in a defect (*). *D*, tooth dentin. (C–F) Serial sections obtained at 10 days were subjected to H&E staining (C) or immunostaining for CD44 (D), TN-C (E) or ALP (F). The panels include the defect area consisting of soft tissue (*) and newly formed bone (*N*) and the endochondral area (*E*) on the original cortex (*C*). The CD44-immunopositive cells (red in D) and TN-C-immunopositive matrices (red in E) remain located in the defect (*). Osteoblasts at the margin of newly formed bone (arrowheads) and chondrocyte precursor cells (arrow) are immunopositive for ALP (brown) but not for CD44. Not counterstained in (B,D–F). Similar results were obtained in three independent experiments. Scale bar represents 200 μ m.

assessment of periodontal regeneration, although the model does not represent a critical size defect (16,21,25–28). In this model, others have transplanted skin fibroblasts genetically modified to express bone morphogenetic protein (BMP) and shown that BMP-transduced fibroblasts promote osteogenesis and cementogenesis, but control-transduced fibroblasts do not (26). Those studies and local delivery of recombinant BMP show endochondral ossification (16,26). In this study, FN-ALP transplants improved the effects of grafted fibroblasts on periodontal healing.

Moreover, to our knowledge, this is the first report of grafted fibroblasts increasing endochondral bone formation in alveolar healing, without genetic manipulation. Our approach avoids the problems of gene therapy (29). Further studies on evaluation of the transplants in more clinically relevant animal models are needed.

The induction of ALP appears relevant to the ability of FN-ALP transplants to heal alveolar bone defects and increase bone formation. Non-ALP transplants (without ALP induction) formed less bone both inside and outside the defect than did

FN-ALP transplants. Unexpectedly, grafted cells ceased ALP expression early in the healing process. Thus, it is unlikely that the graft's ALP directly affects the healing outcome. One possibility is that the induction of ALP in fibroblasts *in vitro* is accompanied by the evolution of other functions, because it requires specific culture conditions, such as mitogen deprivation-induced growth arrest (11,20), that could modify gene expression (30). Little is known about the factors modulating fibroblast ALP expression *in vivo*. We previously showed that the ECM regulates ALP expression by gingival fibroblasts *in vitro*, in that FN enables them to express ALP, whereas collagen fibrils suppress ALP expression and overcome FN (11). Others have shown, using an engineered tissue-like culture, that gingival fibroblasts cease ALP expression as collagen accumulation proceeds (8). Since collagen matrix assembly depends on a preformed FN matrix (31), FN-based transplants may provide a template for collagen deposition early in the healing process.

There are two main possible explanations for how grafted cells contribute to bone formation: one is that the cells differentiate along a chondro-osseous pathway and another is that they stimulate and recruit host cells (32). The former cannot explain the present findings, because we showed that new bones formed by both intramembranous and endochondral ossification in the FN-ALP transplant group are of host origin. We tracked grafted cells by using human-specific mAbs to CD44 and TN-C. Besides fibroblasts, cells of the osteoblast lineage express CD44 (33), a cell-surface glycoprotein interacting with various ECM components (34), and both osteogenic and chondrogenic cells deposit TN-C in the matrix (35). Marker-positive grafted cells/matrices were undetected in newly formed bone and cartilage. They were located near ALP-positive host osteoblasts and chondrocyte precursor cells early in the healing process and were then replaced by host bone tissues. Thus, in our model, FN-ALP transplants recruit host osteo/chondrogenic cells to promote bone formation. We

found no histological signs of graft rejection because of administration of the immunosuppressant FK506 by the established protocol (17,18), which has little influence on rat bone healing (18). Studies have shown that FK506 does not alter fibroblast CD44 expression (36). Thus, the replacement of FN-ALP transplants by host tissues suggests that the grafts are remodeled during the host healing process. It is known that skin substitutes containing fibroblasts, which stimulate wound healing, persist in wounds for a limited period (37). Owing to the short persistence of FN-ALP transplants and their ALP expression *in vivo*, it is possible that the grafts act on host cells during the initial phase of periodontal healing. Further studies on the mechanism of action of FN-ALP transplants are needed.

In conclusion, FN-based, ALP-expressing human gingival fibroblast transplants not only support alveolar regeneration within the defect but also augment bone formation outside the defect through the recruitment of host osteo/chondrogenic cells in a rat periodontal defect model.

Acknowledgements

This work was supported in part by a Grant-in Aid for Scientific Research (C) (15592192) (18592265) from the Ministry of Education, Science, Sports and Culture of Japan.

References

- Pihlstrom BL, Michalowicz BS, Johnson NW. Periodontal diseases. *Lancet* 2005;**366**:1809–1820.
- Bartold PM, Xiao Y, Lyngstaadas SP, Paine ML, Snead ML. Principles and applications of cell delivery systems for periodontal regeneration. *Periodontol* 2000 2006;**41**:123–135.
- Edwards PC, Mason JM. Gene-enhanced tissue engineering for dental hard tissue regeneration: (2) dentin-pulp and periodontal regeneration. *Head Face Med* 2006;**2**:16.
- Taba M Jr, Jin Q, Sugai JV, Giannobile WV. Current concepts in periodontal bioengineering. *Orthod Craniofac Res* 2005;**8**:292–302.
- Benatti BB, Silvério KG, Casati MZ, Sallum EA, Nociti FH Jr. Physiological features of periodontal regeneration and approaches for periodontal tissue engineering utilizing periodontal ligament cells. *J Biosci Bioeng* 2007;**103**:1–6.
- Xiao Y, Qian H, Young WG, Bartold PM. Tissue engineering for bone regeneration using differentiated alveolar bone cells in collagen scaffolds. *Tissue Eng* 2003;**9**:1167–1177.
- Abe T, Akamine A, Hara Y, Maeda K. Expression of membrane alkaline phosphatase activity on gingival fibroblasts in chronic inflammatory periodontal disease. *J Periodont Res* 1994;**29**:259–265.
- Hillmann G, Gebert A, Geurtsen W. Matrix expression and proliferation of primary gingival fibroblasts in a three-dimensional cell culture model. *J Cell Sci* 1999;**122**:2823–2832.
- Hessle L, Johnson KA, Anderson HC *et al*. Tissue-nonspecific alkaline phosphatase and plasma cell membrane glycoprotein-1 are central antagonistic regulators of bone mineralization. *Proc Natl Acad Sci USA* 2002;**99**:9445–9449.
- Murshed M, Harmey D, Millán JL, McKee MD, Karsenty G. Unique coexpression in osteoblasts of broadly expressed genes accounts for the spatial restriction of ECM mineralization to bone. *Genes Dev* 2005;**19**:1093–1104.
- Abe T, Abe Y, Aida Y, Hara Y, Maeda K. Extracellular matrix regulates induction of alkaline phosphatase expression by ascorbic acid in human fibroblasts. *J Cell Physiol* 2001;**189**:144–151.
- Cukierman E, Pankov R, Stevens DR, Yamada KM. Taking cell-matrix adhesions to the third dimension. *Science* 2001;**294**:1708–1712.
- Clark RAF, McCoy GA, Folkvord JM, McPherson JM. TGF- β 1 stimulates cultured human fibroblasts to proliferate and produce tissue-like fibroplasia: a fibronectin matrix-dependent event. *J Cell Physiol* 1997;**170**:69–80.
- Akizuki T, Oda S, Komaki M *et al*. Application of periodontal ligament cell sheet for periodontal regeneration: a pilot study on beagle dogs. *J Periodont Res* 2005;**40**:245–251.
- Hasegawa M, Yamato M, Kikuchi A, Okano T, Ishikawa I. Human periodontal ligament cell sheets can regenerate periodontal ligament tissue in an athymic rat model. *Tissue Eng* 2005;**11**:469–478.
- King GN, King N, Cruchley AT, Wozney JM, Hughes FJ. Recombinant human bone morphogenetic protein-2 promotes wound healing in rat periodontal fenestration defects. *J Dent Res* 1997;**76**:1460–1470.
- Akahane M, Ohgushi H, Yoshikawa T *et al*. Osteogenic phenotype expression of allogeneic rat marrow cells in porous

- hydroxyapatite ceramics. *J Bone Miner Res* 1999;**14**:561–568.
18. Voggenreiter G, Siozos P, Hunkemöller E, Heute S, Schwarz M, Obertacke U. Immunosuppression with FK506 has no influence on fracture healing in the rat. *Bone* 2005;**37**:227–233.
 19. Steenstrup T, Clase KL, Hannon KM. Rapid quantification of cell numbers using computer images. *Biotechniques* 2000;**28**:624–626.
 20. Abe T, Hara Y, Abe Y, Aida Y, Maeda K. Serum or growth factor deprivation induces the expression of alkaline phosphatase in human gingival fibroblasts. *J Dent Res* 1998;**77**:1700–1707.
 21. Lekic P, Sodek J, McCulloch CAG. Osteopontin and bone sialoprotein expression in regenerating rat periodontal ligament and alveolar bone. *Anat Rec* 1996;**244**:50–58.
 22. Macneil RL, Sheng N, Strayhorn C, Fisher LW, Somerman MJ. Bone sialoprotein is localized to the root surface during cementogenesis. *J Bone Miner Res* 1994;**9**:1597–1606.
 23. Minguell JJ, Erices A, Conget P. Mesenchymal stem cells. *Exp Biol Med* 2001;**226**:507–520.
 24. Midwood KS, Williams LV, Schwarzbauer JE. Tissue repair and the dynamics of the extracellular matrix. *Int J Biochem Cell Biol* 2004;**36**:1031–1037.
 25. Lekic PC, Rajshankar D, Chen H, Tenenbaum H, McCulloch CAG. Transplantation of labeled periodontal ligament cells promotes regeneration of alveolar bone. *Anat Rec* 2001;**262**:193–202.
 26. Jin Q-M, Anusaksathien O, Webb SA, Rutherford RB, Giannobile WV. Gene therapy of bone morphogenetic protein for periodontal tissue engineering. *J Periodontol* 2003;**74**:202–213.
 27. Jin Q, Anusaksathien O, Webb SA, Printz MA, Giannobile WV. Engineering of tooth-supporting structures by delivery of PDGF gene therapy vectors. *Mol Ther* 2004;**9**:519–526.
 28. Zhao M, Jin Q, Berry JE, Nociti FH Jr, Giannobile WV, Somerman MJ. Cementoblast delivery for periodontal tissue engineering. *J Periodontol* 2004;**75**:154–161.
 29. Cavazzana-Calvo M, Thrasher A, Mavilio F. The future of gene therapy. *Nature* 2004;**427**:779–781.
 30. Schneider C, King RM, Philipson L. Genes specifically expressed at growth arrest of mammalian cells. *Cell* 1988;**54**:787–793.
 31. Velling T, Risteli J, Wennerberg K, Mosher DF, Johansson S. Polymerization of type I and III collagens is dependent on fibronectin and enhanced by integrins $\alpha_1\beta_1$ and $\alpha_2\beta_1$. *J Biol Chem* 2002;**277**:37377–37381.
 32. Gugala Z, Olmsted-Davis EA, Gannon FH, Lindsey RW, Davis AR. Osteoinduction by ex vivo adenovirus-mediated BMP2 delivery is independent of cell type. *Gene Ther* 2003;**10**:1289–1296.
 33. Jamal HH, Aubin JE. CD44 expression in fetal rat bone: *in vivo* and *in vitro* analysis. *Exp Cell Res* 1996;**223**:467–477.
 34. Ponta H, Sherman L, Herrlich PA. CD44: from adhesion molecules to signaling regulators. *Nat Rev Mol Cell Biol* 2003;**4**:33–45.
 35. Mackie EJ, Thesleff I, Chiquet-Ehrismann R. Tenascin is associated with chondrogenic and osteogenic differentiation *in vivo* and promotes chondrogenesis *in vitro*. *J Cell Biol* 1987;**105**:2569–2579.
 36. Johnsson C, Gerdin B, Tufveson G. Effects of commonly used immunosuppressants on graft-derived fibroblasts. *Clin Exp Immunol* 2004;**136**:405–412.
 37. Jimenez PA, Jimenez SE. Tissue and cellular approaches to wound repair. *Am J Surg* 2004;**187**(suppl):56S–64S.

This document is a scanned copy of a printed document. No warranty is given about the accuracy of the copy. Users should refer to the original published version of the material.